



Article

Energy Absorption in Carbon Fiber Composites with Holes under Quasi-Static Loading

Omar Alhyari and Golam Newaz *

Mechanical Engineering Department, Wayne State University, Detroit, MI 48202, USA; omar.alhyari@wayne.edu

* Correspondence: gnewaz@eng.wayne.edu

Abstract: Composite tubular structures have shown promise as energy absorbers in the automobile industry. This paper investigates the energy absorption characteristics of carbon fiber reinforced plastic (CFRP) tubes with pre-existing holes. Holes may represent an extreme case of impact damage that perforates the tube, e.g., stones from road surface impacting the tubes. Tubes with holes represent more conservative performance characteristics, since impact damage of the same size will have residual material, which may carry some load. Tubes with holes can provide the lower limit of CFRP tube performance under axial crushing relative to impact damaged tubes with perforation diameter close to the hole diameter. In this study, tubes with lay-up of [05/902/04] with one and two holes in defined locations and different diameters are experimentally studied under quasi-static loading. It was found that specific energy absorption (SEA) reduces by 50% with one or two holes of 15 mm size, 100 mm from top of the tube. The SEA reduction is about 60% lower than the regular tube when the diameter of the hole is 20 mm located at 100 mm from top. The most severe reduction occurs if the location of single or double holes are 75 mm from the top. In this case, a SEA reduction of 75% can be expected. Results indicate that holes can significantly alter the energy absorption capability of the tubes. It is also clear that in axial crushing of composite tubes, the location of the hole (100 to 75 mm) appears to create more pronounced effect than the size of the hole itself (15 vs. 20 mm) for the cases investigated. The failure modes for tubes with holes seem to preserve similar damage modes with delamination, frond creation, and brittle fracture, which is typically observed in regular composite tubes under axial crushing load. This is due to primarily front end crushing, which dominates the failure modes, while hole induced damage occurs later.

Keywords: carbon fiber reinforced plastics (CFRP); energy absorption; composite materials; thin walled tubes; damage; quasi-static loading



Citation: Alhyari, O.; Newaz, G. Energy Absorption in Carbon Fiber Composites with Holes under Quasi-Static Loading. *C* **2021**, *7*, 16. <https://doi.org/10.3390/c7010016>

Received: 5 January 2021

Accepted: 22 January 2021

Published: 1 February 2021

Publisher's Note: MDPI stays neutral with regard to jurisdictional claims in published maps and institutional affiliations.



Copyright: © 2021 by the authors. Licensee MDPI, Basel, Switzerland. This article is an open access article distributed under the terms and conditions of the Creative Commons Attribution (CC BY) license (<https://creativecommons.org/licenses/by/4.0/>).

1. Introduction

The Corporate Average Fuel Economy (CAFE) standards and the strong safety standards have forced auto manufacturers to search for materials that can achieve the high strength to weight ratio without manufacturing complexity or increasing the cost. It was well known that traditional materials like steel will not meet the auto industry's requirements, which has led manufacturers to investigate the possibility of using lighter weight composite materials. Recent developments in all aluminum vehicles such as Ford 150 pick-up trucks show a trend to use lightweight materials.

Automakers see an increase in fuel efficiency each time they can reduce the vehicle mass. Auto manufacturers continued looking for ways to achieve higher strength to weight ratios without impacting the safety of the occupants. One of the car components that received attention for achieving significant strength to weight ratio is the use of CFRP energy absorbers in the vehicle frame, as shown in Figure 1. The conventional approach involves the use of steel to manufacture the energy absorbing components such as crush cans behind the bumper, which absorbs energy through controlled collapse by folding and hinging, involving extensive local plastic deformation.

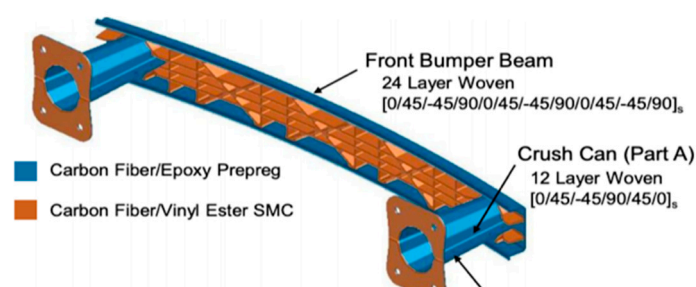


Figure 1. CFRP crush cans attached to composite bumpers [1].

As a result of new developments in composite materials industry, it was clear that the benefits of using composite materials could provide a perfect replacement for traditional materials like steel due to their high strength, stiffness, and low density. Due to more stringent safety legislation, the performance of composite materials during crushes became an important topic for researchers and manufacturers. It may be noted that the crush can be subjected to stone impact from the road. Any damage to the crush can lower its energy absorption capability. Whether they should be replaced due to stone impact creating perforations is the issue being addressed in this article.

The early research investigating the composite materials as crush energy absorption structures began in the mid-1970s. Three pioneering research groups are credited with major contributions establishing a solid understanding of how the composite materials behave and fail under crush loads and absorb energy: Thornton from Ford Motor Co., Hull from University of Cambridge, and Farley from the U.S. Army. Hull [2] was the first who identified three different crushing modes: Type I: a long single central interlaminar crack, whose length is greater than the thickness of the wall of the tube. Type II: a central interlaminar crack, whose length is less than the thickness of the tube wall. Type III: no central interlaminar crack with the tube wall bending outward from the center of the tube. Thornton provided great insight on the crushing mechanism through proper characterization and structural response of tubes under crush loads [3–5]. Farley [6–8] described Type I crushing mode as a lamina bending mode, while the Type II and III modes seem to be a combination of more fundamental crushing modes and geometry-related failure modes.

Thornton [4] reported that tubes made from unidirectional prepreg were found to produce higher energy-absorption capability than woven material. Other researchers like Hamada et al. [9–12] observed increasing the SEAs for a range of high temperature thermoplastic matrices and found a correlation with increasing matrix fracture toughness. Mamalis et al. [13,14] proposed a new method to perform the bending crushing test. Czaplicki et al. [15] reported that the energy absorbed by tulip triggered specimens was significantly higher than bevel triggered ones of the same geometry and material. Abdel Haq et al. studied crushing failure mechanisms in glass fiber tubular structures in detail, which showed similar failure modes as in CFRP tubes [16–18]. Farley [6–8] reported that the static and dynamic tests produced the same energy absorption, but it was reported that composite materials absorbed energy without catastrophic failure of the tubes. Farley also reported that higher strain at failure composite material system exhibited superior energy absorption capability. Farley [6] summarized the characteristics for tubes by four modes: transverse shearing, brittle fracturing, lamina bending, and local buckling, as shown in Figure 2.

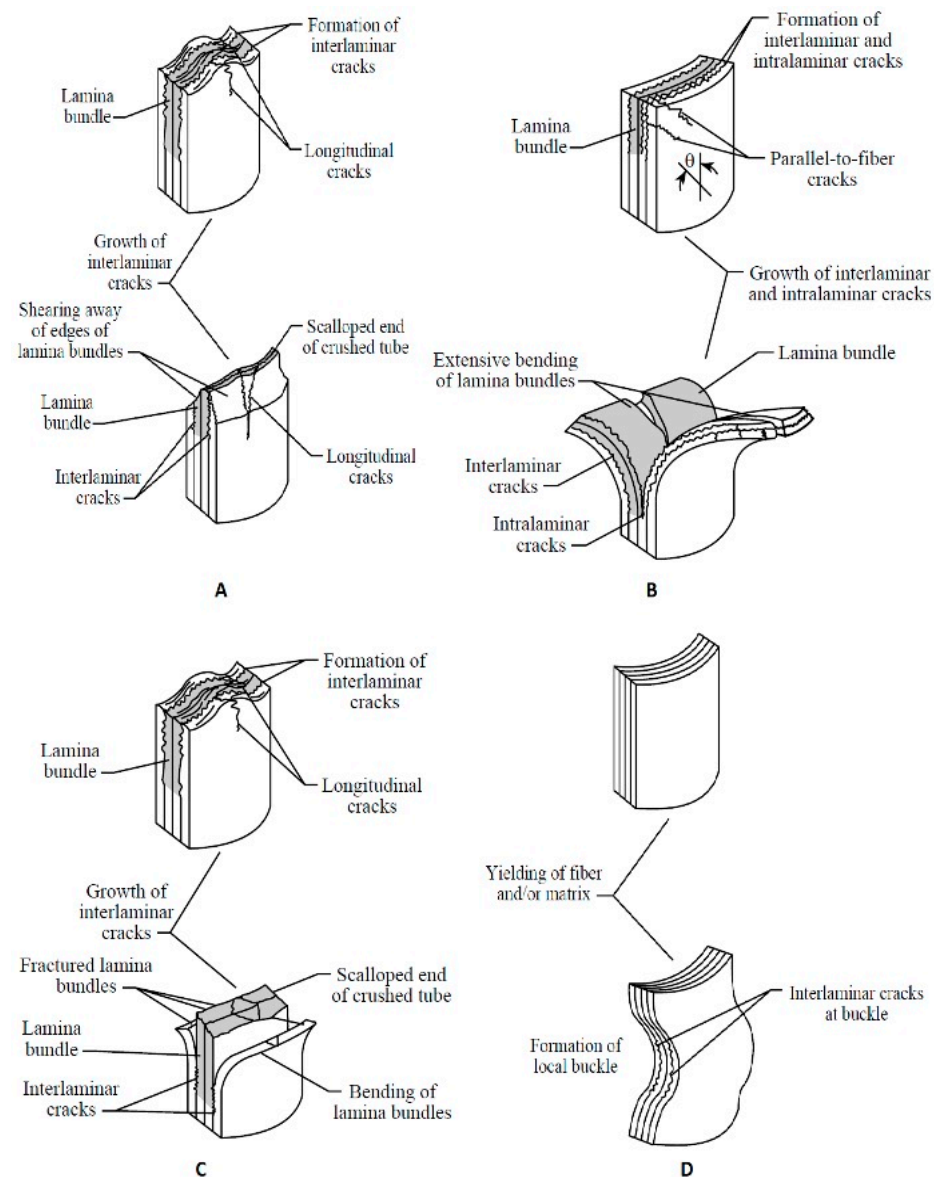


Figure 2. Typical failure modes observed in CFRP tubes under axial crushing [6]. (A–D), represent typical key failure modes that are observed.

Kim et al. [19] reported that for tubes with hybrid unidirectional fibers, the crushing modes were determined by the types of the fibers in the axial direction. Chiu et al. [20] reported that strain rate will not affect the performance of composite structures response to crush loads. Ma et al. [21] concluded that for carbon/aramid CFRP capability of absorbing energy increased after treatment while carbon/carbon CFRP did not show changes in energy absorption after treatment.

These key references point out that when increasing the fiber and matrix stiffness, the energy absorption capability increases. They also explain the effects of the fiber and matrix failure strain on the energy absorption capability.

The specific energy absorption (SEA) is a frequently used parameter to indicate the energy absorption capability, which is defined as the amount of energy, absorbed per unit mass crushed material, and it can be calculated by calculating the area under load-displacement curve, as shown in Figure 3.

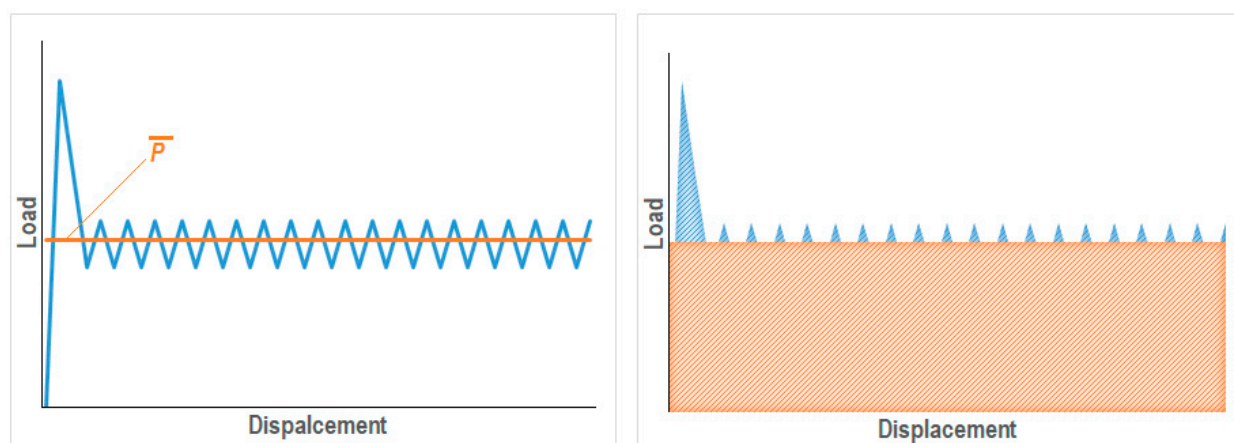


Figure 3. Typical load–displacement curve.

The \overline{P} is the mean crash load and is independent of the crash displacement. The *SEA* can be expressed in Equation (1) [10]:

$$SEA = \frac{\overline{P}}{A \rho} \quad (1)$$

where ρ is the material density, A is the cross-sectional area of the tube, and \overline{P} is the average crush load. The load \overline{P} times the entire displacement, say, d as in the orange rectangle (area under the average crushing load) represents total energy, $\overline{P} \times d$, absorbed by the tube. Dividing the total mass of the crushed portion of the tube is $M = A \cdot d \cdot \rho$ and then canceling d from numerator and denominator results in Equation (1).

The composite materials have anisotropic mechanical properties, which means that damages cause severe degradation, but it is difficult to predict the damage, because it is internal damage. Composites are known to be susceptible to damage caused by transverse loads even under low-velocity impacts. The composites can be damaged on the surface; importantly, they can be damaged below the surface by relatively light impacts causing barely visible damage. A hole or a cutout represents lack of load carrying capability in the axial direction in this local area of the tube akin to localized impact damage area and also serves as a stress concentration factor (SCF) for the composite. Although impact damage is not the same as holes or cutouts, the latter represents a more conservative estimate of the capability of the energy absorber, since in the impact damage case, some material in the damaged area similar to the size of the hole may still transmit load.

Many types of research investigated how circular holes and notches affect the flat composite plates; particularly, Saha et al. did a detailed study [22]. However, studies to find out how holes affect the composite cylinders and tubes are very limited. Initial studies on the effect of holes assumed that the curvature has no or little effect on stress concentration, but the thin shell theory required the shell to have critical length. By using bending and tension tests, it was concluded that a hole will add stresses to the shell if R/a is less than 4, where R is the inner diameter and a is the hole diameter. Van Tooren et al. [23] found that the hole's stress concentration is dependent on curvature. Quinn and Duliéu-Barton [24] confirmed that SCF can be approximated for a hole in the cylinder using flat plate data. SCF for composite analysis has been addressed by Wu and Mu [25]. Liang et al. [26] investigated the curvature effect for cylindrical shell with circular hole under pressure, where they reported that increasing the curved angle will lead to higher resistance to the external pressure load. In our investigation, we do not address strength characteristics due to the SCF in the tube. In this work, our goal is to assess the reduction in energy absorption capability of composite tubes due to macro-defects (holes) present in the tubes in CFRP to gain an understanding of how severely the energy absorption capability is compromised. Novelty for this work is in gaining new knowledge are two-fold: (a) how

energy absorption is affected due to axial crushing of carbon fiber tubes in the presence of holes (macro-defects or discontinuities that may mimic stone impact), where very little understanding is there in open literature, and (b) shedding light on failure mechanisms for such tubes subjected to axial crushing force and checking if they are similar to regular tubes without holes or present other modalities.

2. Experimental Aspects

2.1. Description of CFRP Tube Samples

The composite CFRP unidirectional tubes used in this experimental work were manufactured By Newport Inc. using Toray 700S-12K and Newport 301 epoxy, which is a 250° F to 300° F cure, semi-toughened, controlled flow epoxy resin system. Versatile processing, excellent mechanical properties, and long out-life make Newport 301 suitable for a variety of structural applications. The density of the CFRP material is 1.65 g/cc.

The mechanical properties of the composite are listed in Table 1. The tube geometry is shown in Figure 4; the lay-up is $[0_5/90_2/0_4]$. Each tube has a 45° chamfer end.

Table 1. Mechanical properties of the $[0_5/90_2/0_4]$ CFRP tube.

Tensile Modulus (GPa)	Tensile Strength (MPa)	Comp. Modulus (GPa)	Comp. Strength (MPa)	Flexural Modulus (GPa)	Flexural Strength (MPa)
127	2250	123	1247	98	1500

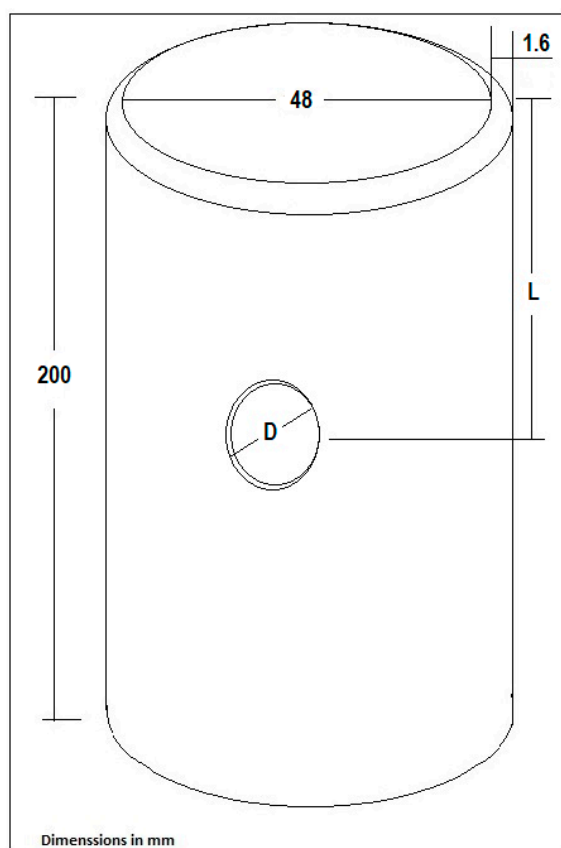


Figure 4. CFRP tube geometry and dimensions in mm.

The CFRP tubes used in these experiments were 200 mm long and 48 mm inner diameter with 1.6 mm in thickness. Tubes with holes were based on hole's location, hole's diameter, and number of holes; tube code 100-15-2 means the hole location is 100 mm from

the chamfered end, hole diameter is 15 mm, and the number of holes is 2. Similarly, holes located 75 mm from top had the designation of 75-15-1, etc. Table 2 provides the average dimensions of the composite tubes. Figure 4 shows the tube geometry and dimensions.

Table 2. Tube sample types and dimensions.

Tube	Length (mm)	L (mm)	D (mm)	No. of Holes	No. of Samples
	200			0	5
100-15-1	200	100	15	1	5
100-15-2	200	100	15	2	5
100-20-1	200	100	20	1	5
100-20-2	200	100	20	2	3
75-15-1	200	75	15	1	5
75-15-2	200	75	15	2	5

2.2. Testing Setup

The composite tubes were tested using 810 MTS universal machine (245 kN) at room temperature. All specimens were crushed about 100 mm at a crosshead rate of 0.5 mm/s. Five repeated experiments were carried out for each set of tests to verify the repeatability of energy-absorption capability, except for the case where two holes of 20 mm dia were located at 100 mm from the chamfered end, which is discussed later. Repeatability of tests provided confidence in testing only three samples for this case only. All tests were run under the displacement-controlled condition.

3. Results and Discussion

The composite tube crushing process is progressive failure by nature, where the chamfered end will trigger the damaging processes when peak force is reached, then a slight decrease to stable crushing force is experienced. Damage spreads progressively throughout the tube. The advantage of this failure process is high energy absorption, because most of the tube is damaged over a large deflection range, while an average crushing force is maintained.

It was established by previous work [2–21] that composite tubes absorbed the energy via progressive damage in different modes. The damage initially starts at the top of the chamfered area where high hoop tensile strain exists, then propagates downwards along the tube wall. The damage propagates along the tube wall, causing the tube wall to split into fronds by matrix splits. In these tubes, the outer ply is 0° ply, which separates from the bulk of the tube and splays outwards due to delamination. With this splaying mode, debris starts falling and creates gaps. The inner-most plies exhibit similar behavior as the outer-most plies, but they splay inwards. In general, the inner plies show substantial damage due to internal constraints, which generate a large amount of debris. The fiber breakage is clearly observed for the 0° and 90° plies. The 0° plies break into smaller pieces compared to 90° plies, but the fragments in the 0° plies are smaller. The overall damage process is shown in Figure 5.

Out of all damage types, the brittle fracture (fiber and matrix separation and fiber breaks in rapid succession) is the main damage. The axial load is carried mainly by the 0° fibers, but the 90° plies will also contribute to it, although axial stiffness for this layer is low. Due to axial loading, the 90° layers bend and break via shearing; these shear conditions are promoted due to relative axial displacement of 0° and 90° plies as a consequence of delamination between the layers. The test results show that crushing involves basic failure modes such as splaying, brittle fracture, and transverse shearing. The failure modes are shown in Figure 5.

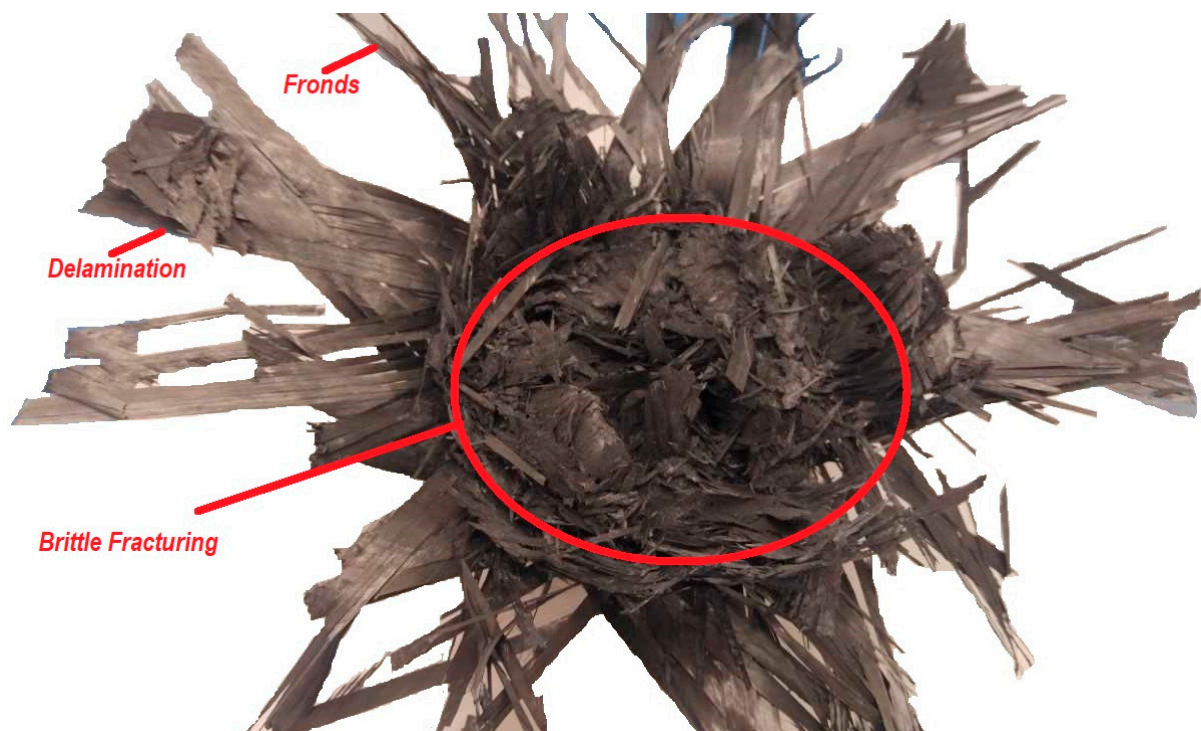


Figure 5. Representative collapse modes of 50 mm dia composite circular CFRP tubes, exhibiting many of the failure modes depicted by Farley [7] for regular CFRP tubes, as shown in Figure 2.

3.1. Response of Regular Tubes without Holes

For the regular tubes with no holes tested in this work, five samples were tested where the crushing behavior and force–displacement curves were quite similar. Using these results, an average curve was generated, as shown in Figure 6.

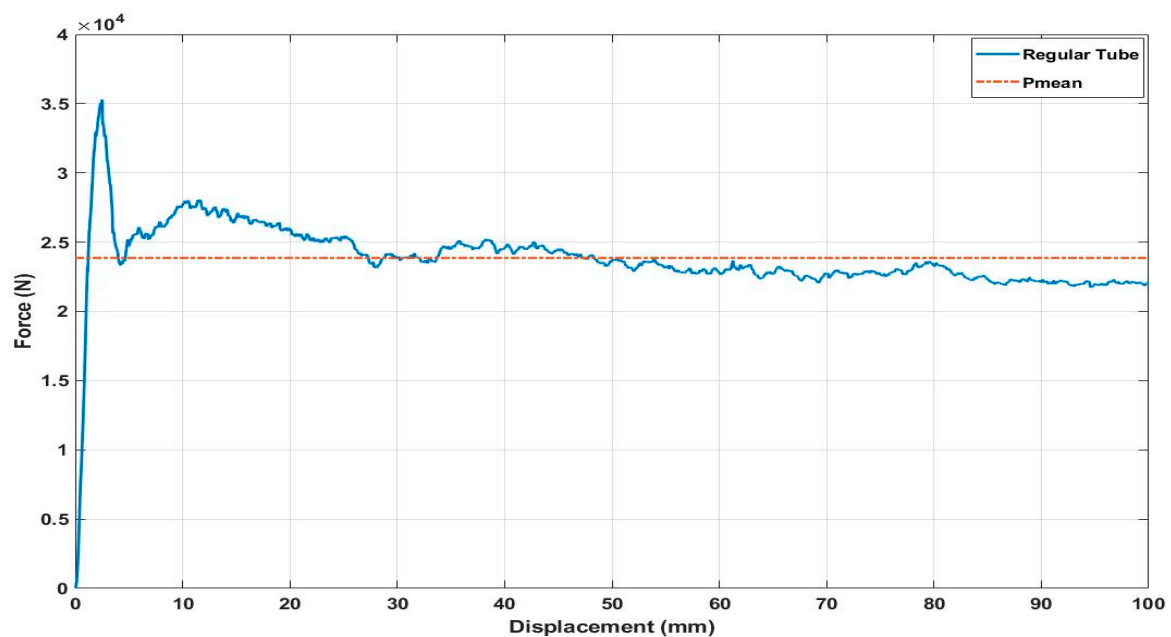


Figure 6. Average force–displacement experimental curve (blue) for the regular tube. The red line represents P_{mean} line for the entire load–deflection response (100 mm of deflection).

The average force–displacement represents the typical force–displacement curve for composite materials. The force will increase until it reaches the peak and then drop to a

lower level and later increase to steady state level until the crash process is completed. The total energy absorption is equal to the area under the force–displacement curve, or by integrating the curve, the specific energy absorption (SEA) can be calculated by using Equation. 1, which is essential to compare the performance of tube material in relation to the weight of the system to show overall load carrying and energy absorption efficiency in relation to material mass. However, the SEA is dependent on the tube’s material, geometry, ply orientation, and matrix. P_{\max} is the peak force, and P_{mean} is the mean or average value of crushing force. This is estimated for the deflection level of 100 mm. Table 3 provides peak force, mean force, energy absorbed, and SEA for the five CFRP tubes tested.

Table 3. Peak force, mean force, and SEA.

Experimental			
P_{\max} (kN)	P_{mean} (kN)	EA (kJ)	SEA (kJ/kg)
35.3 ± 3.25	23.9 ± 0.82	2.39 ± 0.08	57.5 ± 1.93

3.2. Response of Tube with Holes

It is expected that the mode of failure may be altered due to pre-existing holes according to the reported results by Corum et al. [27], who investigated the low energy impact effects on automotive structural composites, where they reported that the strength reduction using compression after impact (CAI) response of carbon fiber laminate due to central circular hole is similar to the strength reduction caused by impacted defects of approximately similar size, the hole providing a more conservative result. In this paper, the strength degradation due to holes was found to provide a reasonable lower bound to the strength degradation caused by impact damage. This result adds credence to the common assumption, often used in damage tolerance evaluations, that impact-induced defects introduce the same strength reduction as a hole of the same size.

Each tube with an existing hole has a threshold size where there is no influence on the progressive crush response below this hole size. If the hole is located at 100 mm, a number of experiments confirmed that threshold diameter is approximately 12 mm; below this diameter size, no appreciable difference was found in P_{\max} and P_{mean} values as long as the hole is located at least 100 mm from the chamfered end. The tubes with pre-existing holes are listed in Table 2. All the tubes are tested under a quasi-static test with 0.5 mm/sec load speed using 810 MTS machine (245 kN).

The samples experienced failure in various modes: the tubes with pre-existing holes started with splaying matching the regular tubes. After reaching the peak force, the tubes damaged via progressive failure. At a greater deflection level, cracks initiate at the hole, causing the tube to split and collapse. Hole initiated cracks propagate quickly and in sudden bursts. Once the platen contacts the dense damaged material pack, the load rises again due to debris compaction. This stage is not useful, as the tube has already collapsed and also does not contribute to energy absorption.

The presence of a hole makes the tube weaker at the point when the cracks initiate from the holes and cause load drops, and thus the absorbed energy will be less than the regular tube. This result matches what Karbhari et al. [28] reported, that post impact will cause a reduction in energy absorption by composite materials and the crush performance will change. It is observed that until the failure initiation from the crack, the peak p value (Figure 7), and the overall mean value, P_{mean} are not affected much. This clearly shows that if the location of the hole is removed away from the load application point, then original characteristics of energy absorption and P_{mean} may be preserved for the tube until precipitous load drop, when cracking at the hole dominates the tube response. Figure 7 is showing the damage as a function of the force–displacement curve at three points: A represents the P_{peak} , B represents the start of the steady state force, and C represents when the crack is initiated by the pre-existing hole. At Cm it is noted that the 15 mm circular hole is no longer circular due to the crack initiation.

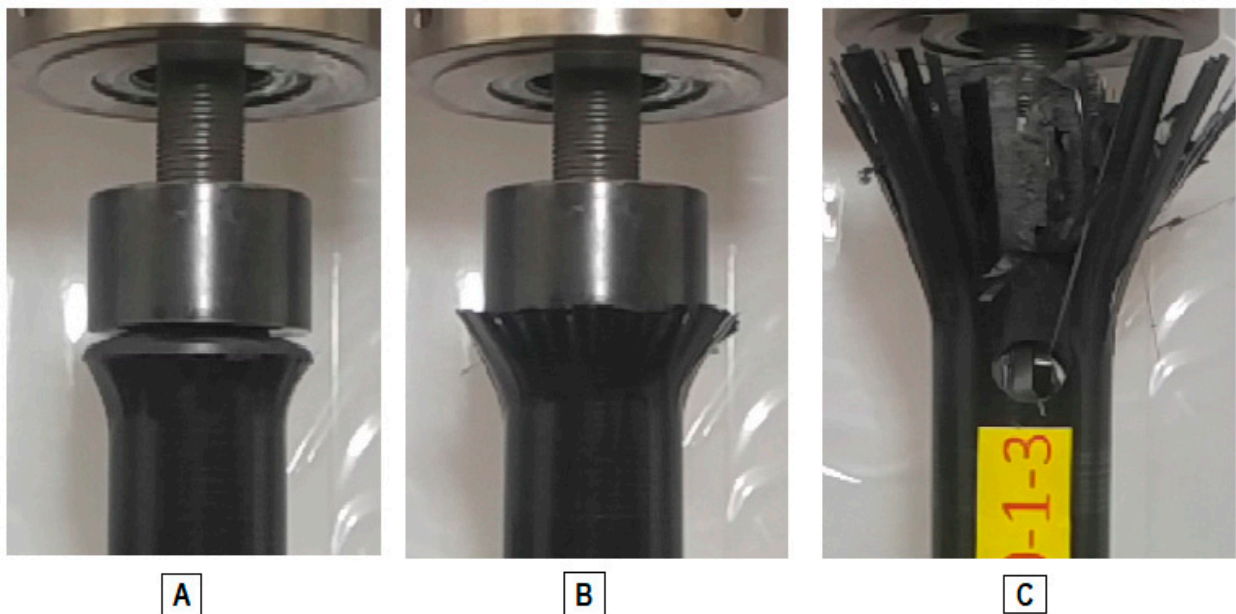
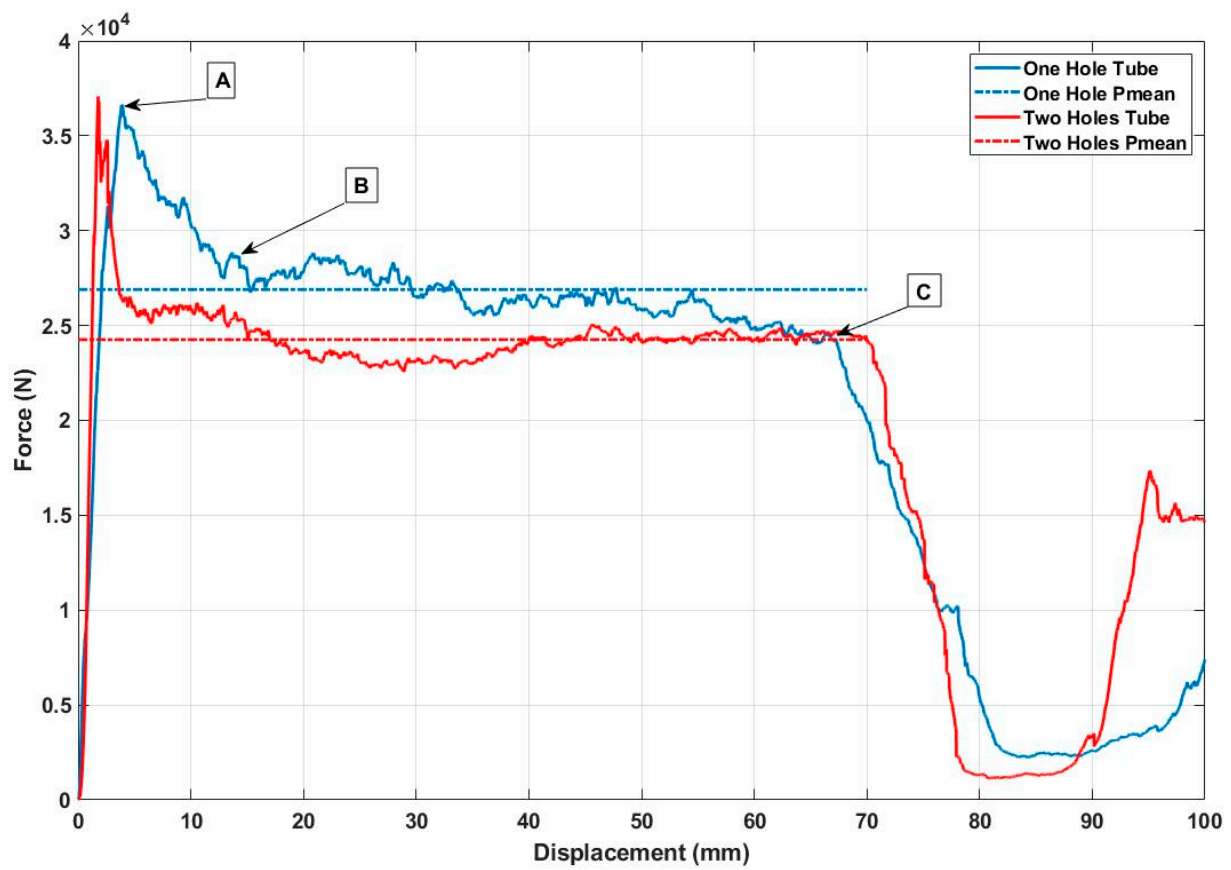


Figure 7. Force–displacement curves for the tubes with 15 mm hole, 100 mm from chamfered top (average).

The response of the tube for single hole vs. two holes is shown in Figure 7. The curves are average of five tests. One notes that the P_{mean} value for the two-hole tube is somewhat lower than the single-hole sample response. In addition, the precipitous drop in load carrying capability of the tube occurs around 70 mm vertical deflection. For the samples with 20 mm holes, the P_{mean} values (Figure 8) are lower than the 15 mm hole samples (Figure 7). Another important feature is that with larger hole size of 20 mm, the precipitous

load drop occurs a little earlier at 66 mm deflection level compared to samples with 15 mm holes at 70 mm deflection level (compare Figures 7 and 8).

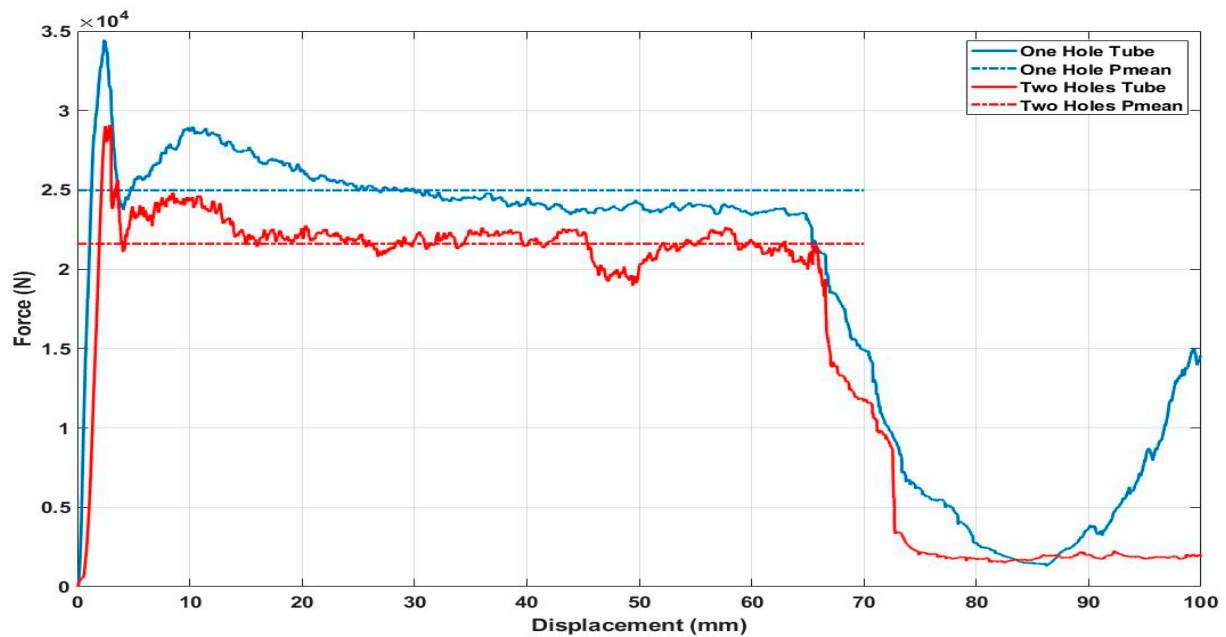


Figure 8. Force–displacement curves for the Tubes with 20 mm hole, 100 mm from chamfered top (average).

Figure 9 represents the load–displacement curves for the average results obtained from tubes with pre-existing 15 mm holes at 75 mm distance from the chamfered end. It is interesting to note that the location of the holes being closer from the top location of the tube have similar response and P_{mean} are very similar. However, the precipitous load drop occurs at about 50 mm of vertical deflection, much earlier than when the holes are 100 mm from the chamfered end. The force displacement curves for tubes with preexisting holes for the six tubes tested in this work showed same trend; the force will increase until it reaches the peak and drop to steady state level, and significantly drop when the crack is initiated by the hole and propagated around the circumference. P_{max} , P_{mean} , energy absorbed, and SEA are obtained from experimental data are listed in Table 4.

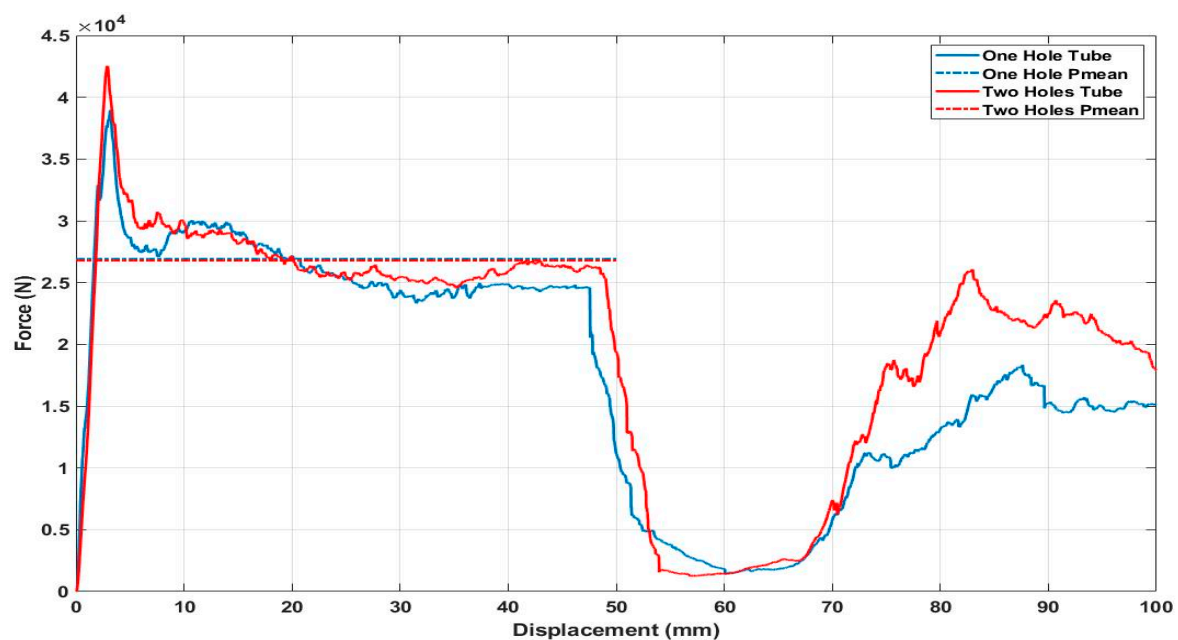


Figure 9. Force–displacement curves for the tubes with 15 mm hole, 75 mm from chamfered top (average).

Table 4. SEA and other data for tubes with holes.

Tube	Experimental				
	P_{\max} (kN)	P_{mean} (kN)	Energy (kJ)	SEA kJ/kg	% of Regular Tube SEA
100-15-1	36.6 ± 4.50	26.9 ± 1.85	1.82 ± 0.19	29.96 ± 2.7	52.1
100-15-2	37.1 ± 5.34	24.3 ± 1.17	1.71 ± 0.12	29.40 ± 2.3	51.1
100-20-1	34.4 ± 2.50	25.0 ± 1.34	1.63 ± 0.14	25.81 ± 2.0	44.9
100-20-2	29.1 ± 3.80	21.6 ± 0.95	1.43 ± 0.03	22.96 ± 1.5	39.9
75-15-1	39.0 ± 3.30	26.1 ± 0.50	1.24 ± 0.07	14.30 ± 0.6	24.9
75-15-2	42.5 ± 1.50	26.8 ± 0.96	1.30 ± 0.08	15.48 ± 1.2	26.9

The results listed in Table 4 show that the number of holes and the hole diameter did not play a significant role in the energy absorption capability of the tubes. For the tubes with one 20 mm hole located at 100 mm from the chamfered top, the drop in SEA is 7.2%, compared to a tube with one 15 mm hole located 100 mm from the chamfered top. Additionally, it is noted that the number of holes did not have dramatic effect on energy absorption. The tube with two 15 mm holes located 100 mm from the chamfered top has lower SEA by 0.26 kJ/kg compared to a tube with one 15 mm hole. The highest effect was caused by the hole location, where we can observe that the SEA for tubes with 15 mm hole located 75 mm from the chamfered top is approximately 50% of the SEA for tube with 15 mm hole located 100 mm from the chamfered top. In our review of even most recent papers in open literature, we find this important issue of presence of defects has not been addressed [29–32]. Our results provide some new information in this area that is relevant for application of these tubes for energy absorption in automotive applications.

4. Conclusions

In this study, the crashworthiness performance of CFRP composite tubes with and without pre-existing holes have been investigated experimentally. The work focused on the effect of holes on the energy absorption under quasi-static load in the tubes.

It was observed that tubes without holes crushed progressively with stable performance. The tube splayed, and long fronds were created, and small debris formation was observed. The tubes with pre-existing holes displayed similar failure modes as observed in tubes without holes until the damage progressed closer to the hole when the tube splayed and long fronds were created. When the load reached a critical point, a crack at the hole will be formed where the stress was the highest and then propagate around the circumference quickly. The crack leads to significant damage, which will cause the tube to split and collapse. It was found that specific energy absorption (SEA) reduces by 50% with one or two holes of 15 mm size, 100 mm distance from top of the tube. The SEA reduction is about 60% lower than the regular tube when the diameter of the hole is 20 mm located at 100 mm from top. The most severe reduction occurs if the location of single or double holes are 75 mm from top. In this case, a SEA reduction of 75% can be expected. Results indicate that holes can significantly alter the energy absorption capability of the tubes. It is also clear that in axial crushing of composite tubes, the location of the hole (100 to 75 mm) appears to create more pronounced effect than the size of the hole itself (15 vs. 20 mm) for the cases investigated. The failure modes for tubes with holes seem to preserve similar damage modes with delamination, frond creation, and brittle fracture, which are typically observed in regular composite tubes without holes under axial crushing load.

Author Contributions: O.A.: investigation, data curation and writing—original draft preparation; G.N.: writing—review and editing, supervision. All authors have read and agreed to the published version of the manuscript.

Funding: The research received no external funding.

Conflicts of Interest: The authors declare no conflict of interest.

References

1. Coppola, T.; Faruque, O.; Board, D. Validation of Material Models for Crash Simulation of Automotive carbon Fiber Composite Structures. In Proceedings of the Society of Plastics Engineers (SPE)—American Society for Composites (ACC) Meeting, East Lansing, MI, USA, 6 September 2017.
2. Hull, D. A Unified Approach to Progressive Crushing of Fiber Reinforced Composite Tubes. *Compos. Sci. Technol.* **1991**, *40*, 377–421. [\[CrossRef\]](#)
3. Thornton, P.H.; Jeryan, R.A. Crash Energy Management in Composite Automotive Structures. *Int. J. Impact Eng.* **1988**, *7*, 167–180. [\[CrossRef\]](#)
4. Thornton, P.H. Energy Absorption of Composite Structures. *J. Compos. Mater.* **1979**, *13*, 247–262. [\[CrossRef\]](#)
5. Thornton, P.H. The Crush Behavior of Pultruded Tubes at High Strain Rates. *J. Compos. Mater.* **1990**, *24*, 594–615. [\[CrossRef\]](#)
6. Farley, G.L. Energy Absorption of Composite Materials. *J. Compos. Mater.* **1983**, *17*, 267–279. [\[CrossRef\]](#)
7. Farley, G.L. Effect of Fiber and Matrix Maximum Strain on the Energy Absorption of Composite Materials. *J. Compos. Mater.* **1986**, *20*, 322–334. [\[CrossRef\]](#)
8. Farley, G.L. Effect of Specimen Geometry on the Energy Absorption Capability of Composite Materials. *J. Compos. Mater.* **1986**, *20*, 390–400. [\[CrossRef\]](#)
9. Hamada, H.; Ramakrishna, S. Effect of Fiber Material on the Energy Absorption Behavior of Thermoplastic Composite Tubes. *J. Thermoplast. Compos. Mater.* **1996**, *9*, 259–279. [\[CrossRef\]](#)
10. Ramakrishna, S.; Hamada, H.; Maekawa, Z.; Sato, H. Energy Absorption Behavior of Carbon-Fiber-Reinforced Thermoplastic Composite Tubes. *J. Thermoplast. Compos. Mater.* **1995**, *8*, 323–344. [\[CrossRef\]](#)
11. Hamada, H.; Ramakrishna, S.; Sato, H. Effect of Fiber Orientation on the Energy Absorption Capability of Carbon Fiber/PEEK Composite Tubes. *J. Compos. Mater.* **1996**, *30*, 947–963. [\[CrossRef\]](#)
12. Hamada, H.; Ramakrishna, S. Scaling Effects in the Energy Absorption of Carbon-Fiber/PEEK Composite Tubes. *Compos. Sci. Technol.* **1995**, *55*, 211–221. [\[CrossRef\]](#)
13. Mamalis, A.G.; Manolacos, D.E.; Viegela, G.L. Crashworthy Behavior of Thin-Walled Tubes of Fiberglass Composite Material Subjected to Axial Loading. *J. Compos. Mater.* **1990**, *24*, 72–91. [\[CrossRef\]](#)
14. Mamalis, A.G.; Manolacos, D.E.; Demosthenous, G.A.; Ioannidis, M.B. The Deformation Mechanism of Thin-Walled Non-Circular Composite Tubes Subjected to Bending. *Compos. Struct.* **1995**, *30*, 131–146. [\[CrossRef\]](#)
15. Czaplicki, M.J.; Robertson, R.E.; Thornton, P.H. Comparison of Bevel and Tulip Triggered Pultruded Tubes for Energy Absorption. *Compos. Sci. Technol.* **1991**, *40*, 31–46. [\[CrossRef\]](#)
16. Abdel-Haq, M.; Newaz, G.M. Role of Failure Modes on Energy Absorption in Unidirectional PMC Tubes. *J. Compos. Mater.* **2001**, *35*, 941–953. [\[CrossRef\]](#)
17. Abdel-Haq, M.; Newaz, G.M. Influence of Crush Mechanisms on Energy Absorption of PMC Square Tubes. *J. Thermoplast. Compos. Mater.* **2001**, *14*, 160–174. [\[CrossRef\]](#)
18. Abdel-Haq, M.; Broggiato, G.B.; Newaz, G.M. Constraint Effects on Energy Absorption in Unidirectional PMC Tubes. *J. Compos. Mater.* **1999**, *33*, 774–793. [\[CrossRef\]](#)
19. Kim, J.S.; Yoon, H.J.; Shin, K.B. A study on Crushing Behaviors of Composite Circular Tubes with Different Reinforced Fibers. *J. Impact Eng.* **2011**, *38*, 198–207. [\[CrossRef\]](#)
20. Chiu, L.N.S.; Falzon, B.G.; Ruan, D.; Xu, S.; Thomson, R.S.; Chen, B.; Yan, W. Crush Responses of Composite Cylinder under Quasi-static and Dynamic Loading. *Compos. Struct.* **2015**, *131*, 90–98. [\[CrossRef\]](#)
21. Ma, Y.; Sugahara, T.; Yang, Y.; Hamada, H. A study on the energy absorption properties of carbon/aramid fiber filament winding composite tube. *Compos. Struct.* **2015**, *123*, 301–311. [\[CrossRef\]](#)
22. Saha, M.; Prabhakaran, R.; Waters, W.A., Jr. Compressive Behavior of Pultruded Composite Plates with Circular Holes. *Compos. Struct.* **2004**, *65*, 29–36. [\[CrossRef\]](#)
23. Van Tooren, M.J.L.; Van Stijn, I.P.M.; Beukers, A. Curvature Effects on the Stress Distribution in Sandwich Cylinders with a Circular Cut-Out. *Compos. Part A* **2002**, *33*, 1557–1572. [\[CrossRef\]](#)
24. Quinn, S.; Dulieu-Barton, J.M. Determination of Stress Concentration Factors for Holes in Cylinders using Thermoelastic Stress Analysis. *Blackwell Sci. Strain* **2002**, *38*, 105–118. [\[CrossRef\]](#)
25. Wu, H.-C.; Mu, B. On Stress Concentrations for Isotropic/Orthotropic Plates and Cylinders with a Circular Hole. *Compos. Part B* **2003**, *34*, 127–134. [\[CrossRef\]](#)
26. Liang, C.C.; Hsu, C.Y.; Chen, W. Curvature Effect on Stress Concentrations around Circular Hole in Opened Shallow Cylindrical Shell under External Pressure. *Int. J. Press. Vessel. Pip.* **1998**, *75*, 749–763. [\[CrossRef\]](#)
27. Corum, J.M.; Battiste, R.L.; Ruggles-Wren, M.B. Low-Energy Impact Effects on Candidate Automotive Structural Composites. *Compos. Sci. Technol.* **2003**, *63*, 755–769. [\[CrossRef\]](#)
28. Karbhari, V.M.; Haller, J.E.; Falzon, P.K.; Herszberg, I. Post-impact crush of hybrid braided composite tubes. *Int. J. Impact Eng.* **1999**, *22*, 419–433. [\[CrossRef\]](#)
29. Chambe, J.E.; Bouvet, C.; Dorival, O.; Ferrero, J.-F. Energy absorption capacity of composite thin-wall circular tubes under axial crushing with different trigger initiations. *J. Compos. Mater.* **2020**, *54*, 1281–1304. [\[CrossRef\]](#)

-
30. Palanivelu, S.; Van Paepegem, W.; Degrieck, J.; Van Ackeren, J.; Kakogiannis, D.; Van Hemelrijck, D.; Wastiels, J.; Vantomme, J. Experimental study on the axial crushing behaviour of pultruded composite tubes. *Polym. Test.* **2010**, *29*, 224–234. [[CrossRef](#)]
 31. Emadi, M.; Beheshti, H.; Heidari-Rarani, M. Multi-Objective Optimization of Hybrid Aluminum–Composite Tube Under Axial Crushing. *Int. J. Appl. Mech.* **2020**, *12*, 2050042. [[CrossRef](#)]
 32. Hwang, S.-F.; Chang, Y.-C. Axial Crushing Behavior of Braided Carbon/Polyurethane Composite Tubes. *Appl. Compos. Mater.* **2019**, *26*, 1281–1297. [[CrossRef](#)]